

Experimental Study of the Combustion Dynamics of a Bluff Body Stabilized Methane Flame in Ducted Combustor

ChanYeong Jeong, Jinhyun Bae, Taesung Kim, Youngbin Yoon
Seoul National University
Jet Propulsion Laboratory
599 Gwanak-ro, Gwanak-gu, Seoul, KOREA

Abstract

The flame dynamics were investigated in the ducted combustor with the V-gutter bluff body. The combustor has a long duct shape with a cross-section area of 40 mm x 40 mm. Natural Gas was used as fuel, which was injected transversely into the cross-flow. In order to study flame characteristics related to longitudinal combustion instability, various measurement techniques were applied such as direct-photography, dynamic pressure measurement, OH radical chemiluminescence, and particle image velocimetry (PIV). The flashback distance from the edges of a bluff body and flame changes and unstable flames can be classified into three types. In particular, when the backflow flame goes over the bluff body, a circular flame occurs at the front of the bluff body. In the event of flashback, as combustion pressure downstream increases, inlet air cannot go through the bluff body; the flame front moves along the sides of the bluff body in order to react with the fuel-air mixture. Re-stabilization takes place as the flame moves downstream. This process is supported by a strong vortex structure, which is a result of the velocity difference between the stagnant flow behind a bluff body and the outer shear flow passing through a bluff body.

Nomenclature

m_a inlet air mass flow

t^* time variation from the start of the one period
 ϕ equivalence ratio
MFC Mass Flow Controller
RMS Root-mean-square

Introduction

A bluff body has been used to stabilize the flame in air-breathing propulsion engine. When the influx air velocity is very high, the bluff body produces recirculation zone flow behind it to hold a flame. Since the research of Zukoski [1] and Roshko [2] was published, numerous studies have been carried out in order to understand the flow characteristics and combustion stabilization that occur near the bluff body [3-6]. The flow characteristics of the bluff body are affected by its geometric properties, such as size, shape, blockage ratio, dimension, and array. They are also affected by influx flow characteristics in front of the bluff body. These characteristics determine not only the static properties such as pressure, temperature, velocity, and combustion efficiency, but also determine the flame stabilization and flame blowoff. Previously, because the objective of the bluff body is to anchor and stabilize the flame, many studies focused on flame stabilization and blowoff.

Therefore, combustion instability near the bluff body has been investigated, particularly hydrodynamic instability and thermo-acoustic instability. Much of the research about blowoff is related to hydrodynamic instability

[7,8]. However, few studies have investigated thermo-acoustic instability in the combustor using a bluff body. Since the 1980s, a lot of research has dealt with longitudinal combustion instability caused by thermo-acoustic interaction in gas turbine engines and ramjet engines. In the case of gas turbine engines, the research results are well summarized in the literature [9-11].

In addition, the research of flame dynamics near the bluff body has been continuously conducted from until now. Yu et al. [12] investigated low-frequency pressure oscillations in a model dump ramjet combustor. They revealed that the instability is associated with large-scale flame-front motions that are driven by periodic vortex shedding at the instability frequency. Recently, from the study reported by Wright et al. [13], researchers such as Langhorne [14], Bloxidge et al. [15], Dowling [16], and Shanbhogue et al. [7] have discussed the flame dynamic and flame stability near bluff body.

As stated, many studies have discussed the mechanism of longitudinal combustion instability in various combustors, particularly dump and side-dump combustors. However, this research is insufficient to fully understand the longitudinal mode of a bluff body in confined combustor.

Furthermore, this lack of the research is in the flashback phenomenon. Flashback is very complex phenomenon when the oxidizer and fuel is premixed. The cause of the flashback is mentioned in various papers [17]. Sommerer et al. briefly described a variety of reason into divided five categories [18]. Among these, the flashback occurring in the confined combustor with bluff body is due to 'the flashback by combustion instability'. In 1980s, the experimental studies of flashback were conducted in the bluff body and rearward facing step [19,20]. And, Dowling [16], Thibaut and

Candel [21] carried out the analytic and numerical studies. However, their research was focused on the relatively weak flashback, and the strong flashback that the flame moves over the bluff body has not been made many studies. It is required a complete understanding to the flashback because there is a possibility of serious damage to the upstream of the combustor that is vulnerable to heat.

Therefore, the basic characteristics of the longitudinal combustion instability are conducted on the confined combustor. And the flame structure was visualized by OH radicals and PIV method when the flame moves upstream over the bluff body to investigate the flashback.

Experimental Apparatus and Conditions

A. Experimental Apparatus

In this study, a lab-scale model combustor was used with a v-gutter bluff body (Fig. 1). The combustor has a square cross-section area of 40 mm x 40 mm and a long duct shape in the longitudinal direction. An air compressor used to supply influx air can deliver compressed air up to 8 bars. An orifice having a diameter of 5 mm denoted the upper acoustic boundary of the combustor. Fuel was the natural gas composed of 89% methane and 9% ethane. Fuel was injected perpendicular to the air flow direction with two plane-orifice injectors mounted at the top and bottom of the mixing section. The injectors were located at 830 mm ahead of the bluff-body in the combustion section. Air and fuel mass flow rates was controlled by the MFC.

A torch igniter uses hydrogen and air and was installed directly below the bluff body. The V-gutter bluff body takes the shape of an equilateral triangle, the sides of which are 14 mm in length. The 20 mm thick quartz windows was used in order to transmit the laser and

visualize the flame. These windows were installed at the top and side of the combustion section. At the end of the extension duct, a nozzle was installed to make a fixed acoustic length. The nozzle has a square cross-section area of 40 mm x 20 mm.

For analysis, the NI PXI-1042 system and the NI USB-6218 BNC have been used to acquire temperature, static pressure, and dynamic pressure. Also, a K-type thermocouple (Omega Co.), a pressure transducer (Valcom Co.), the Model 102A05 (PCB INC.) were respectively used to measure the temperature, static pressure, dynamic pressure information. The sampling rate of temperatures and static pressures was 1 Hz. Dynamic pressure data were obtained at 5,000 samples per second.

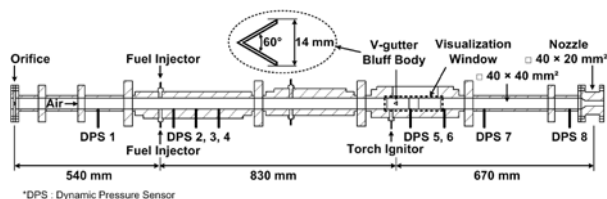


Figure 1. Schematic of the ducted combustor with the bluff body

B. Experimental Conditions

In this study, both sensor-based and image-based methods were applied. First, eight dynamic pressure sensors were mounted at the combustor using the infinite tube method. Using these sensors, dynamic pressure signals were simultaneously measured at various locations of the combustor. And combustion frequencies and pressure fluctuations were then obtained from the signal processing. Second, to observe the structure and change of the flame, image-based methods were used such as direct photography, particle image velocimetry (PIV), and OH radical chemiluminescence using an intensified charge-coupled device (ICCD) high-speed camera (FASTCAM Ultima II, Photron Co.) because

these radicals are proportional to heat-release fluctuations. PIV signals were emitted by the sheet beam produced by the composition of double pulse PIV laser (Nd:YAG laser, 532 nm) and cylindrical lenses. Zirconium oxide with a mean diameter of about 1 μm was used as a seeding particle. These signals were captured using a CCD camera (Princeton ES2020, 1600 X 1200). The images were taken to obtain high accuracy spontaneous velocity profiles and these images were processed using a commercial program (TSI Insight 3G). An ICCD high-speed camera with a 105 mm macro lens (Canon) was used to evaluate the flame structure according to the phase of combustion instability. It had a resolution of 512 x 256 pixels and a frame rate set to 10000 fps. A trigger signal was used to adjust the accurate timing signal between the high-speed ICCD camera image and the dynamic pressure signal. The 310 mm band-pass filter with 10 nm bandwidth located in front of the high speed ICCD camera detected OH radical chemiluminescence. Combustion tests were performed under various inlet air mass flow rates (m_a) conditions from 10 g/s to 25 g/s m/s by steps of 2.5 g/s. Inlet air and fuel temperature was 290 \pm 1 K. The equivalence ratio (Φ) was controlled between 0.45 and 1.1. Table 1 shows the dimensions of the experimental conditions and combustor design parameters.

Results and Discussion

First of all, we introduce the flame structure of a bluff-body mounted in a ducted combustor and discuss how this type of flame behaves once longitudinal combustion instabilities occur. In order to grasp the flame dynamics occurring in the combustor, flammable ranges were measured for various the air mass flow rates and the equivalence ratios.

Figure 2 is a graph of the stability map. The X-axis represents Φ and the Y-axis represents the m_a . The stability map is divided into four different regions by the change of flashback distance and the flame structure; stable flame, back-flow flame not arriving at the front of a bluff body (A type unstable region), back-flow flame moving over the front of the bluff body (B type unstable region), and back-flow flame with strong flashback and reattachment (C type unstable region). In this paper, flashback distance is defined as the furthest flame moving distance from the tips of a bluff body when the flame moved front of the bluff body during one period of the structural changes of the flame. In Fig. 2, it is found that 1) the unstable flame region is much broader than the stable flame region 2) the B type unstable region takes place within broad range of inlet air velocities and equivalence ratios.

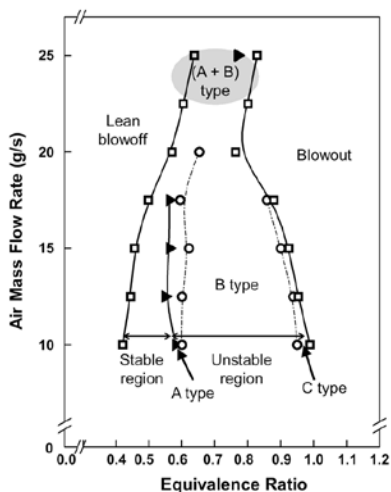


Figure 2. The stability map for various inlet conditions

Figure 3 shows the chemiluminescence images of the stable and unstable flames near the bluff body during one period, which flame-types are classified in Fig. 2. If the combustion instability occurs, flame repeatedly undergoes the flashback and re-stabilization.

Accordingly, one period is selected from a stable flame to the next stable flame. Figure 3(a) shows a typical bluff-body flame, stretched symmetrically at the upper and lower edges of the bluff body, with the forms of the attached flame or lifted flame. The stable flame fluctuates a little due to hydrodynamic instability. Figure 3(b) shows the back-flow flame, which does not arrive at the front of the bluff body. The flame front does not pass over the bluff body but fluctuates between the edges and sides of the bluff body. The back-flow flame going over the bluff body shows a remarkably different flame shape, seen in the Fig. 3(c). When this type of flame occurs, the flame moves in the windward direction and reaches to a distance corresponding to several times the length of the bluff body. This image also shows another flame is increasing at the front of the bluff body and this flame has become the criterion that distinguishes the region of the unstable flames. Figure 3(d) shows the back-flow flame with strong flashback and reattachment. In the case of this flame, the flow moves upstream quickly and detaches from the bluff body completely.

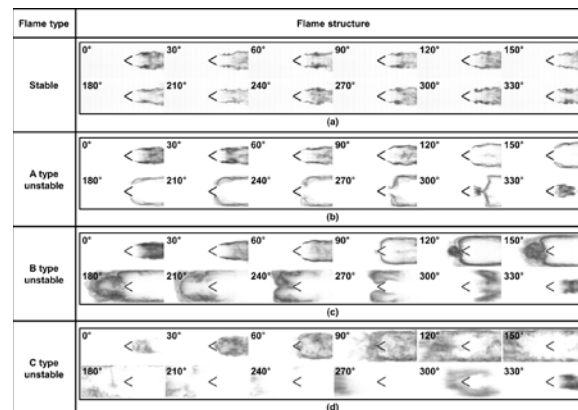


Figure 3. The OH* chemiluminescence images of the stable and unstable flames near the bluff body during one period

Figure 4 shows the magnitude of the dynamic pressure with equivalence

ratio by each air mass flow rate. The dynamic pressure signal is measured at the dynamic sensor nearest to the upper orifice and the magnitude is calculated by the RMS (Root-mean-square) method. Also, the flame regions mentioned above are expressed in all graphs. In Fig. 4(a), the magnitude of the dynamic pressure is relatively small in stable region and rapidly increases at transition point to A type unstable region. This tendency is continued until the moment of the B type unstable region occurs. And the magnitude of the dynamic pressure is maintained similar intent in the B type unstable region. After that, the magnitude steeply increases when the C type unstable region arise. It can be found that changing pattern of the magnitude of the dynamic pressure appeared similar in the various air mass flow rates (Fig. 4(b), 4(c)).

Generally the pressure fluctuation varies in proportion to the combustion instability and the intent of the instability is proportional to the equivalence ratio. In A type unstable region it can be observed that the intent of the instability increases with increasing equivalence ratio. However, in B type unstable region the dynamic pressure has almost constant magnitude despite the increase of equivalence ratio. This phenomenon is regarded as the effect of the new flame which is developed at the front of the bluff body and found only in the B type unstable region. This new heat release source will interact with the existing heat release source, it is considered that the pressure oscillation has a value independent of equivalence ratio. A detailed analysis of the interaction is beyond the scope of this paper and will be achieved through further research. Consequently, it is found that 1) the new flame has a decisive effect on a constant magnitude of the dynamic pressure

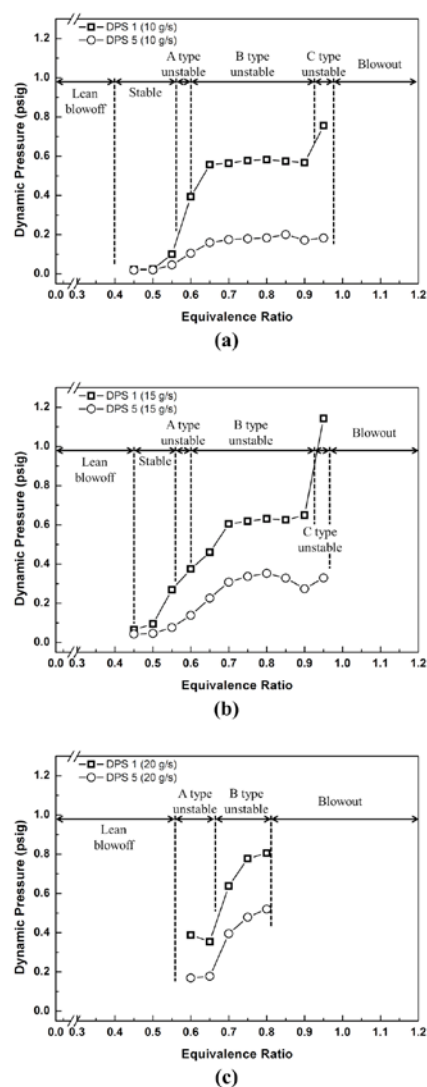


Figure 4. The magnitude of the dynamic pressure with equivalence ratio at (a) $m_a = 10$ g/s, (b) $m_a = 15$ g/s, (c) $m_a = 20$ g/s

in B type unstable region 2) the classification of flammable ranges based on the dynamic pressure in combustor draw a similar conclusion from the classification of flammable ranges based on the structural change of the flame. The above-mentioned descriptions mean we should determine the causes that result in the fluctuating flame near the bluff body, especially for the case of B type unstable region.

Figure 5 shows images that are a combination of the instantaneous PIV and OH radical chemiluminescence images. Figure

5(a) shows the PIV image of the 101° phase of combustion instability cycle. Due to sudden pressure increases downstream, back-flow occurs in the center of the combustor. Because of this, the normal direction flow exists in front of the flame, while there is the back-flow behind the flame. The flame front also moves upstream along the side of the bluff body. Next, the vortex occur perpendicular to the flow at the flame front when the flow from upstream collides with the reverse flow. As a result, the other reverse flow occurs on the front side of the bluff body, while the flame did not reach the same position. Figure 5(b) shows the PIV image of the 130° phase of combustion instability cycle. As can be seen in 5(a), the strong reverse flow exists with the flame front on the side the bluff body. Also, it can then be seen the flow is almost stationary at the position where the new flame collides with the flame on the side of the bluff body. The pressure created by the expansion of the new flame and the pressure coming from downstream cancel each other out, and consequently the flow becomes stationary. Because of this, the flame moving along the side of the bluff body no longer moves forward, but stops.

The new flame occurred in the B type unstable region is associated with the boundary layer in the vicinity the bluff body. When the bluff body is in a flow, a flow velocity on the surface of the bluff body is relatively slower than other region because of the boundary layer on the bluff body. Therefore, it is expected that flame preferentially propagate along the boundary layer on the side of the bluff body. Fig. 6 is the post-processing OH chemiluminescence images that could be regarded as the flame front. In the figure, t^* is the time variation from the start of the one period. When the flame moves

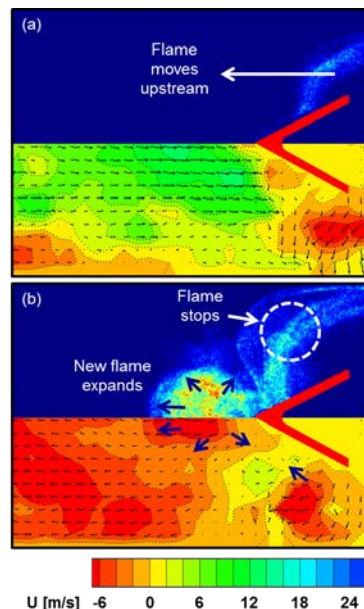


Figure 5. The combination images of the instantaneous PIV and OH radical chemiluminescence at (a) the 101° phase of instability cycle, (b) the 130° phase of instability cycle

upstream, the flame which perpendicularly propagates to the flow has a velocity approximately 6 m/s (indicated by the dash-dotted line). On the other hand, the flame which propagates along the side of the bluff body has a velocity of approximately 16 m/s (indicated by solid line). Thus, at the same time, it can be known that the side flame moves about 2.5 times faster than other flames. Also, vortex was observed on the bluff body side because the mixture-flow collided with the back-flow. This brings about lagging velocity of the mixture and helps the flame to propagate along the side of the bluff body faster than others. Thereby, the flame structure of the B type unstable region is appeared since the mixture of the front of the bluff body ignites first. Consequentially, boundary layer on the bluff body side plays an important role in making characteristic phenomenon of the flame structure.

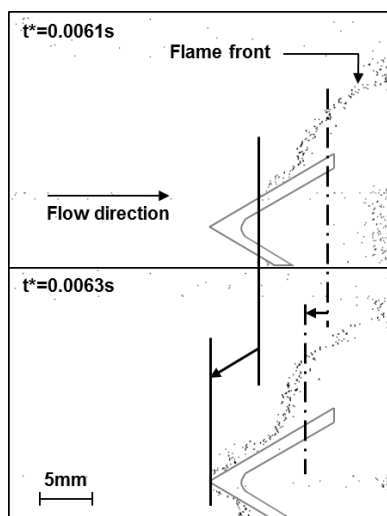


Figure 6. The post-processing OH* chemiluminescence images in the event of the flashback case

Conclusion

Our aim in this study is to understand flame dynamics, especially flashback, of the v-gutter bluff body and to discuss how they occur. Based on our experimental results, the following conclusions are drawn.

First, we investigated flame behavior under condition of longitudinal combustion instability using photography and dynamic pressure measurement. Unstable flames are classified into three types based on the difference of the flashback distance and structural change of the flame. And the same result can be derived with the measurement of the dynamic pressure magnitude. When the back-flow flame goes over the bluff body, it was observed a new circular flame occurring at the front of the bluff body. This phenomenon is regarded to play important role in classification of the flame.

Second, we investigated the flashback processes using dynamic pressure signals, OH radical chemiluminescence and particle image velocimetry. In the event of flashback, as combustion pressure downstream increases, inlet air could not go through the bluff-body

and the flame front, which is located along the balancing surface between the flame propagation speed and the inlet air velocity, moves along the sides of the bluff body in order to react with the fuel-air mixture.

Acknowledgments

This work was supported by National Research Foundation of Korea(NRF) grant funded by Korea government(MSIP) (No. 2015R1A2A2A010043) and the New & Renewable Energy Core Technology Program(201195101001C) of the KETEP grant funded by the MOTIE.

References

1. E.E. Zukoski, "Flame Stabilization on Bluff Bodies at Low and Intermediate Reynolds Numbers", Ph.D.Thesis, 1954.
2. A. Roshko, "On the Development of Turbulent Wakes from Vortex Streets", Report NACA TN 2913, CA, 1953.
3. J.P. Longwell et al., "Flame Stability in Bluff Body Recirculation Zones", Industrial & Engineering Chemistry, 1953.
4. S. Yamaguchi et al., "Structure and blow-off mechanism of rod-stabilized premixed flame", Combustion and Flame, 1985.
5. B. Kiel et al., "A Detailed Investigation of Bluff Body Stabilized Flames", 45th AIAA Aerospace Sciences Meeting and Exhibit, 2007.
6. S.M. Bush et al, "Reacting and Nonreacting Flowfields of a V-Gutter Stabilized Flame", AIAA Journal, 2007.
7. S.J. Shanbhogue et al, "Lean blowoff of bluff body stabilized flames: Scaling and dynamics", Progress in Energy and Combustion Science, 2009.

8. T. Lieuwen et al, "Dynamics of Bluff Body Flames near Blowoff", 45th AIAA ASME, 2007.
9. S. Chaudhuri et al, "Blowoff dynamics of bluff body stabilized turbulent premixed flames", Combustion and Flame, 2010.
10. J. Kariuki et al, "Measurements in turbulent premixed bluff body flames close to blow-off", Combustion and Flame, 2012.
11. J.R. Dawson et al, "Visualization of blow-off events in bluff-body stabilized turbulent premixed flames", Proceedings of the Combustion Institute 33, 2011.
12. K.H. Yu et al., "Low-frequency pressure oscillations in a model ramjet combustor", Journal of Fluid Mechanics, 1991.
13. F.H. Wright et al., "Flame spreading from bluff-body flameholders", Symposium (International) on Combustion, 1961.
14. P.J. Langhorne, "Reheat buzz: an acoustically coupled combustion instability. Part 1. Experiment", Journal of Fluid Mechanics, 1988.
15. G.J. Bloxsidge et al, "Reheat buzz: an acoustically coupled combustion instability. Part 2. Theory", Journal of Fluid Mechanics, 1988.
16. A.P. Dowling, "A kinematic model of a ducted flame", Journal of fluid mechanics, 1999.
17. A. Nauert et al., "Experimental analysis of flashback in lean premixed swirling flames: conditions close to flashback", Experiments in Fluids, 2007.
18. Y. Sommerer et al., "Large eddy simulation and experimental study of flashback and blow-off in a lean partially premixed swirled burner", Journal of Turbulence, 2004.
19. J.O. Keller et al., "Mechanism of Instabilities in Turbulent Combustion Leading to Flashback", AIAA Journal, 1982.
20. L. Vaneveld et al., "Secondary Effects in Combustion Instabilities Leading to Flashback", AIAA Journal, 1984.
21. D. Thibaut et al., "Numerical Study of Unsteady Turbulent Premixed Combustion: Application to Flashback Simulation", Combustion and Flame, 1998.